Nine exceptional radiations plus high turnover explain species diversity in jawed vertebrates

Michael E. Alfaro[a,1], Francesco Santini[a], Chad Brock[b], Hugo Alamillo[b], Alex Dornburg[c], Daniel L. Rabosky[d,e], Giorgio Carnevale[f], and Luke J. Harmon[g]

[a]Department of Ecology and Evolutionary Biology, University of California, Los Angeles, CA 90095; [b]School of Biological Sciences, Washington State University, Pullman, WA 99164; [e]Department of Ecology and Evolutionary Biology and [d]Cornell Laboratory of Ornithology, Cornell University, Ithaca, NY 14850; [f]Dipartimento di Scienze della Terra and Museo di Storia Naturale e del Territorio, Università di Pisa, Pisa, 56100 Italy; [g]Department of Biology, University of Idaho, Moscow, ID 83843; and [c]Department of Ecology and Evolutionary Biology, Yale University, New Haven, CT 06520

Edited by David M. Hillis, University of Texas, Austin, TX, and approved June 12, 2009 (received for review November 2, 2008)

The uneven distribution of species richness is a fundamental and unexplained pattern of vertebrate biodiversity. Although species richness in groups like mammals, birds, or teleost fishes is often attributed to accelerated cladogenesis, we lack a quantitative conceptual framework for identifying and comparing the exceptional changes of tempo in vertebrate evolutionary history. We develop MEDUSA, a stepwise approach based upon the Akaike information criterion for detecting multiple shifts in birth and death rates on an incompletely resolved phylogeny. We apply MEDUSA incompletely to a diversity tree summarizing both evolutionary relationships and species richness of 44 major clades of jawed vertebrates. We identify 9 major changes in the tempo of gnathostome diversification; the most significant of these lies at the base of a clade that includes most of the coral-reef associated fishes as well as cichlids and perches. Rate increases also underlie several well recognized tetrapod radiations, including most modern birds, lizards and snakes, ostariophysan fishes, and most eutherian mammals. In addition, we find that large sections of the vertebrate tree exhibit nearly equal rates of origination and extinction, providing some of the first evidence from molecular data for the importance of faunal turnover in shaping biodiversity. Together, these results reveal living vertebrate biodiversity to be the product of volatile turnover punctuated by 6 accelerations responsible for >85% of all species as well as 3 slowdowns that have produced ''living fossils.'' In addition, by revealing the timing of the exceptional pulses of vertebrate diversification as well as the clades that experience them, our diversity tree provides a framework for evaluating particular causal hypotheses of vertebrate radiations.

evolutionary radiation | macroevolution | phylogeny

The extremes of vertebrate richness have long fascinated evolutionary biologists (1, 2). Species richness of some groups, like teleosts, ostariophysans, birds, mammals, and frogs, is often attributed to accelerated diversification accompanying ecological adaptive radiation or the acquisition of key innovations (3). In contrast, the evolutionary stasis exhibited by many representatives of the sparest branches, such as tuataras, coelacanths, and the bowfin, has been attributed in part to historically low rates of cladogenesis (4, 5). However, the hypothesis that differential diversification rates explain vertebrate biodiversity has rarely been tested. It is possible that, with regard to species richness, some or many of the classic vertebrate radiations might not be exceptional at all. This is because simple models of lineage origination and extinction are expected to produce clades of varying sizes (6). Testing hypotheses about diversification rate at broad phylogenetic scales is challenging for at least 2 reasons. First, most comparative studies of diversity focus on patterns within major clades rather than across them (7–9). Second, most current diversification methods perform best with reasonably well sampled phylogenies, and we are still unable to produce and manipulate densely sampled trees with tens of thousands of tips. Comparative methods like SymmeTREE (10, 11) are an exception to some degree, because they can deal with missing taxa through random resolution of tip clades. However, this approach quickly becomes impractical as the number of unsampled taxa grows.

Here, we analyze a phylogenetic dataset with exemplars of 47 major vertebrate lineages using a comparative method that integrates both phylogenetic and taxonomic information to ask two general questions about the patterns of diversification across the vertebrate tree of life: (*i*) What is the background tempo of vertebrate diversification; and (*ii*) which, if any, vertebrate lineages have patterns of extant richness that are too species-rich or -poor to be outcomes of the background diversification rate?

Results

The diversity tree (Fig. 1), based on divergence time analysis of RAG1 sequence data for 217 jawed vertebrates [gnathostomes; supporting information (SI) Fig. S1–S2, *SI Text*, Tables S1–S7] summarizes phylogenetic and taxonomic information to reveal both the timing of major phylogenetic splits and the average rate of diversification within unresolved lineages. Many gnathostome clades have relatively recent origins, with the 6 most species-rich stem lineages originating in the last 300 million years (Myr) and the top two, modern birds (Neoaves; 9,191 species) and percomorph fishes (Percomorpha; 15,493 species) appearing within the last 175 Myr (Fig. 1).

We tested whether simple models of diversification were good explanations of species richness patterns in living vertebrates using 2 models: a pure-birth (PB) model with one parameter, b, representing the per-lineage rate of speciation; and a birth-death model (BD) with 2 parameters, b and d, representing per-lineage rates of speciation and extinction, respectively (12, 13). The PB model produced a low average rate of diversification for vertebrates (b = 0.059 lineages per Myr, lnL = −768.5), which poorly explained the standing diversity of extant clades: almost all of the 47 lineages in our study have either too many or too few species, given their age, to be plausible outcomes under this model. Using a BD model, we estimated high rates of both speciation and extinction (b = 5.05, d = 5.04, lnL = −611.6). This model showed a substantially better fit to the data compared with the PB model (likelihood ratio test, $\Delta = 313.8$, $P = 3 \times 10^{-70}$). The BD model fit more of the young species-rich stem lineages but

Author contributions: M.E.A. and L.J.H. designed research; M.E.A., F.S., C.B., H.A., A.D., G.C., and L.J.H. performed research; M.E.A., D.L.R., and L.J.H. contributed new analytic tools; M.E.A., F.S., C.B., A.D., and L.J.H. analyzed data; and M.E.A., F.S., C.B., H.A., A.D., D.L.R., G.C., and L.J.H. wrote the paper.

The authors declare no conflict of interest.

This article is a PNAS Direct Submission.

Freely available online through the PNAS open access option.

[1]To whom correspondence should be addressed. E-mail: michaelalfaro@ucla.edu.

This article contains supporting information online at www.pnas.org/cgi/content/full/0811087106/DCSupplemental.

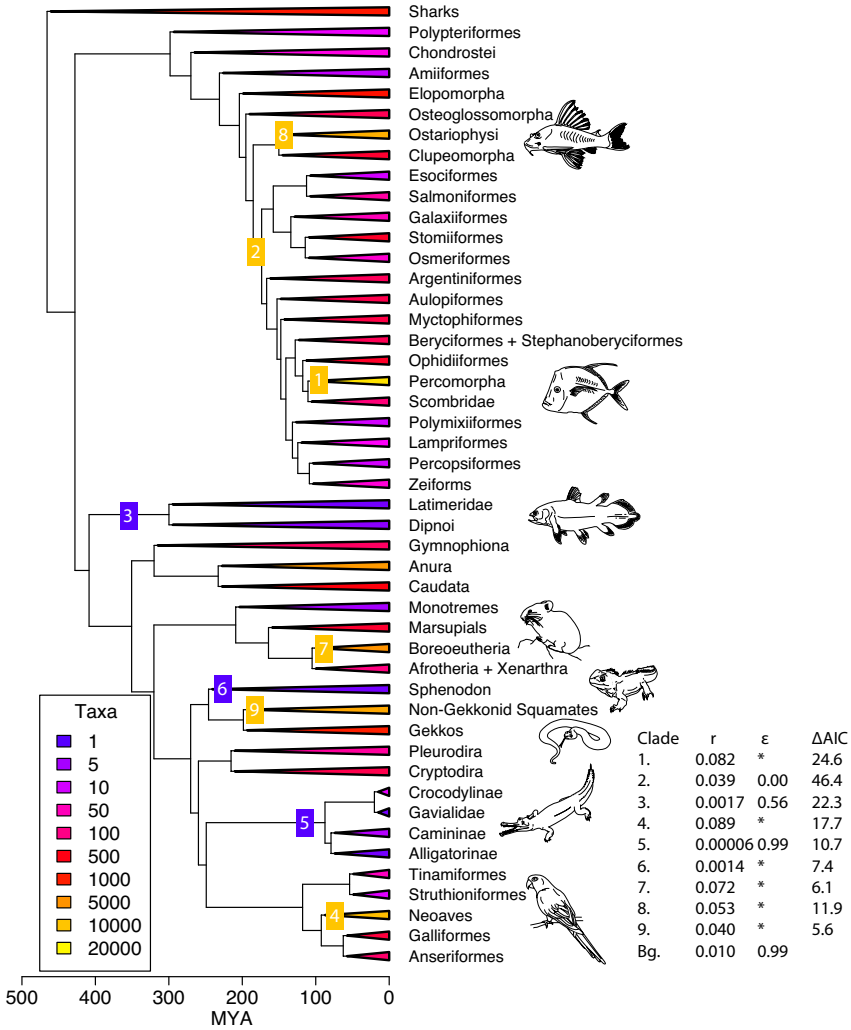

Fig. 1. Diversity tree for analyses of lineage diversification in vertebrates. Clades are collapsed to 47 representative stem lineages and colored by extant species diversity. Clades with unusual diversification rates are denoted with numbers that indicate the order in which rate shifts were added by the stepwise AIC procedure; yellow and blue squares denote diverse and impoverished clades, respectively, compared with background rates. Estimates for net diversification rate ($r = \lambda - \mu$) and relative extinction rate ($\varepsilon = \mu/\lambda$) are included in the lower right table. Relative extinction can be calculated only when at least part of the subclade is resolved [see Rabosky et al. (13)]. Asterisks indicate subclades where ε values could not be estimated for this reason.

offers little improvement in the prediction of low diversity lineages.

To test whether any of the branches of the vertebrate diversity tree led to clades of exceptional species richness given the general BD model, we applied a new comparative method called Modeling Evolutionary Diversification Using Stepwise Akaike Information Criterion (AIC) (MEDUSA; see *Methods and Materials*). We report two main results. First, the background tempo of diversification for large sections of the gnathostome tree of life is characterized by a low overall net rate ($r = 0.010$ lineages/Myr) but also high turnover where the death rate is 99% of the birth rate (Fig. 1). Second, we found 9 periods in vertebrate history where the tempo of diversification changes. The most significant of these are in a subclade of spiny-rayed fishes that we refer to as "percomorphs." This group contains over half of the total diversity of teleosts, including most of the coral-reef-associated fish families as well as freshwater clades like cichlids and perches. We found rate increases leading to 5 other clades as well: most modern birds (Neoaves), 2 large clades of fish (Euteleostei and Ostariophysi), eutherian mammals excluding sloths, anteaters, and related lineages (Boreoeutheria), and non-geckkonid squamates. We also detected 3 significant rate decreases on branches leading to coelacanths (Latimeridae) + lungfishes (Dipnoi), crocodylians, and tuataras (*Sphenodon*).

Discussion

Vertebrate biologists have long held intuitions that the spectacular diversity of many tetrapod groups (teleosts, mammals, birds, and frogs) deserves special explanation. Our method provides a framework for quantitatively testing whether these long-recognized groups really are unexpectedly species rich or poor given their age. In addition, by clarifying the phylogenetic position, magnitude, and the timing of shifts in diversification, analysis with MEDUSA provides a framework for evaluating causal links to diversity. For example, several traits, including hair, mammary glands, and molar characters (14), have been cited as key innovations to explain mammals species richness. Our analysis suggests that an event or series of events within boreoeutherians may be a better explanation for this pattern (Fig. 1, rate shift 7), although the difference in AIC score between placing rate shift 7 on boreoeutherians vs. all mammals does not reject traditional key innovation hypotheses outright ($\Delta AIC_{\text{boreoeutherians vs. all mammals}} \approx 3$). Similarly, although feathers

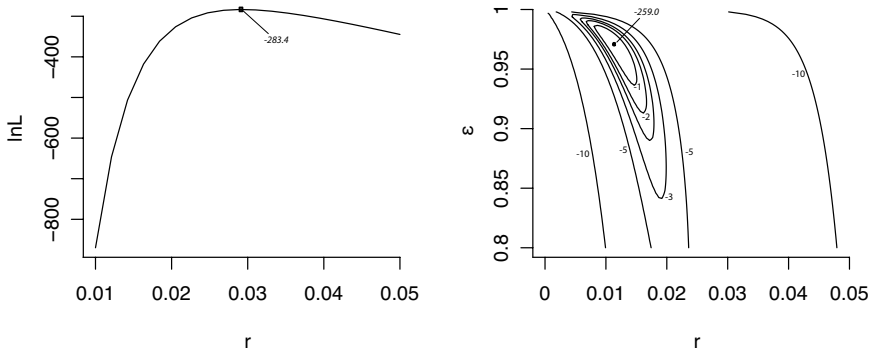

Fig. 2. Likelihood surface for net diversification rate ($r = \lambda - \mu$) and relative extinction rate ($\varepsilon = \mu/\lambda$) for the ''background'' group of vertebrates (see Fig. 1) under PB (*Left*) and BD models (*Right*). Maximum likelihood (ML) estimates are indicated with circles; in *Right*, contours represent models that are varying log-likelihood units below the ML solution.

are cited as a key innovation to explain the radiation of birds (15), our analysis (Fig. 1, rate shift 4) weakly favors the hypothesis that their biodiversity arose from one or more pulses of diversification within the Neoaves ($\Delta AIC_{\text{Neoaves vs. all birds}} \approx 1$).

Our analysis also suggests that frogs may not represent an exceptional vertebrate radiation, at least with regard to their overall species diversity. Allowing a rate shift on anurans does marginally improve the AIC score (*SI Text*), but this improvement is below 4, the threshold level for moderate support (16). This means that the observed species richness of anurans (≈5,500 species) is not much higher than would be expected given the age of their split from salamanders and the background rate of vertebrate diversification. This is not to say that anuran subclades have not diversified especially quickly, or that there have not been periods of rapid anuran cladogenesis (9) but rather that over broad time scales, we should sometimes expect to see large clades produced by a BD process.

One limitation of our approach is that rate shifts cannot be assigned below the level of phylogenetic resolution. For example, the rate shift along the branch leading to Neoaves (Fig. 1, shift 4) might be driven by rapid diversification of perching birds or song birds (or one or more subclades within these groups) rather explosive diversification of Neoaves at large. A related point is that the lack of a rate shift along a branch leading to an unresolved part of the phylogeny does not necessarily imply that subclades within that group have not experienced exceptionally rapid or slow diversification. For example, although the species richness of anurans is not exceptional given their stem age, it is possible that the diversification rate of crown neobatrachians (not examined here because of insufficient taxonomic sampling), which originate well after crown anurans (9) and contain >96% of the species richness of living frogs, could be significantly faster than the background vertebrate rate. Improved sampling of any particular large-scale phylogeny will provide greater power for MEDUSA to more precisely locate diversification rate shifts. We suggest that our method provides one avenue for testing broad-scale macroevolutionary hypotheses, with 2 caveats: (*i*) rate changes in unresolved parts of the tree might be more tipward than they appear, and (*ii*) MEDUSA cannot detect the presence or absence of rates shifts within unresolved parts of the tree. At the scale of relationships among major gnathostome lineages, our study reveals that ≈85% of all living vertebrates have their origins in clades with faster-than-average diversification rates. This highlights the importance of rate shifts in shaping biodiversity, an idea suggested by Simpson (17).

The other main deviations from our constant-rate model are the prototypical ''living fossil'' lineages, old lineages with few extant species (17, 18). In our study, 3 living fossil lineages are notable for both their low rate of speciation and extremely low rates of extinction. These groups stand out in stark contrast to the rest of the vertebrate tree, which is characterized by high rates of both speciation and extinction (Fig. 2). This highlights one of the key challenges presented by living fossils to molecular-based studies of extant diversity: although young species-rich groups can be explained by a transient increase in net diversification rates for a relatively short period, older species-poor groups require negligible rates of both speciation and extinction over tremendously long periods of time to explain their persistence (4, 8, 19–21). We note that all 3 slowly evolving lineages were historically more diverse than they are today (22–24), and that our model is not able to make use of this information. For example, halecomorph fishes (of which the bowfin *Amia calva* is the only surviving member) were a very diverse group during most of the late Mesozoic and into the Paleogene. The family Amiidae, one of 3 major halecomorph lineages, contained at least 27 species during this time and declined rapidly after the Paleogene (25). The true evolutionary history of halcomorphs might thus have involved one or more bouts of increased rates of cladogenesis and extinction. Because MEDUSA does not incorporate any fossil data when fitting rates to explain the standing diversity of halecomorphs, these historical patterns of diversification cannot presently be recovered by our method. Instead, we attempt to find the best BD process that will result in the standing diversity of living halecomorphs (one species) given the age of this lineage. Further development of methods that integrate fossil data with molecular phylogenies (26) will be needed to more thoroughly capture historical dynamics and develop a holistic view of vertebrate diversification.

After our model accommodates exceptionally diversifying clades by assigning them lineage-specific birth and death rates, we find a highly volatile background of vertebrate diversification (b = 0.37, d = 0.36; Fig. 2). Turnover has been shown to play an important role in shaping patterns of fossil diversity in large vertebrate clades [e.g., mammals (5, 27)]. However, although it is theoretically possible to detect extinction rates from molecular phylogenies alone (28), simulation studies on relatively small phylogenies (tens to hundreds of taxa) suggest these estimates have high variance (29). In contrast, our analysis, which captures major diversification events that lead to the evolution of tens of thousands of species, recovers a relatively sharp likelihood surface for estimates of the composite parameters b-d and d/b (Fig. 2). In the context of our BD model, this evidence for turnover comes from the simultaneous presence of young species-rich groups (which can be formed only by high birth rates) and old species-poor groups (whose richness has been depleted by extinction) on the phylogeny. We suggest that integrating taxonomic richness data with phylogenetic trees can provide the phylogenetic breadth needed to detect turnover rates, and that

this is far more challenging at local scales for trees with "only" hundreds of tip species. Improvement to our birth and death estimates might be gained by extending our models to accommodate the observation that diversification in many higher level taxa appears to slow with time (30).

Broad-scale macroevolutionary hypotheses about lineage diversification are often challenging to test. Here, we present a general approach that allows for the integration of taxonomic data that has been collected for centuries with more recently derived backbone phylogenies for sections of the tree of life. Along with providing a quantitative comparative framework for studying diversification at broad scales, MEDUSA can generate new hypotheses and help evaluate causal explanation of radiations. Our study of jawed vertebrates also reveals 2 general patterns, both of which are consistent with a wide range of fossil and comparative data. First, speciation and extinction rates are roughly equivalent at the broadest temporal and taxonomic scales, so that the history of clade diversification is characterized by high turnover. Second, diversification rates vary tremendously among lineages: some of the most species-rich groups in the gnathostomes are amazingly young, whereas other species-poor groups are quite old. Together, these 2 general patterns explain much of the variation in species richness across the vertebrates.

Materials and Methods

Phylogenetic Analyses. Recombination activating gene 1 (*RAG1*) is a well characterized, long, single copy gene that has been widely sequenced across major vertebrate groups (31–36). We downloaded *RAG1* sequences from GenBank for 217 gnathostome species (Table S1). Most of the tetrapod sequences in our dataset were taken from a recent study of divergence times by Hugall et al. (32), whereas the actinopterygian and shark data came from a variety of sources. We used Clustal (37) to create an initial alignment based on amino acid sequences, which we subsequently refined by eye. The master alignment revealed that most tetrapods sequences were substantially longer than the available nontetrapod sequences. To maximize overlap between teleosts and tetrapods and minimize the effects of missing data on our analysis, we trimmed the *RAG1* alignment to 1,445 sites. We then performed a phylogenetic analysis of the data using BEAST (38). We constrained the monophyly of 41 clades so that their origin could be time calibrated using the fossil record (*SI Text*, Table S2). Preliminary analysis of this matrix revealed low effective sample sizes even after 50 million generations for many parameters, as well as several polytomies for well recognized taxonomic groups, suggesting that the Markov chain Monte Carlo (MCMC) chain was not adequately sampling from the target posterior distribution. To improve the behavior of the MCMC sampler, we constrained an additional 31 nodes across the tree that were well supported (PP $\geq$0.90) in the Hugall et al. (32) analysis and/or were widely recognized by standard taxonomical references (see Table S3). There were no cases where these additional constraints conflicted with well supported clades in the preliminary results. We assigned fossil calibrations using lognormal priors with hard lower bounds that reflected the minimum age of the fossil in questions and soft upper bounds where the 95% cumulative probability reflected other relevant information from the fossil record (*SI Text*, Table S2). We estimated divergence times under these topological and temporal constraints where each codon position was assigned a separate GTR + I + G model. To ensure that the chain reached stationarity, we performed 4 separate analyses of the data with 100 million generations each and discarded the first 20 million generations as burnin. Visual inspection of traces within and across runs as well as effective sample sizes >200 for all parameters, performed in Tracer 1.4, suggested our replicate analyses were adequately sampling the target joint distribution. We used the maximum clade credibility tree in our subsequent analysis.

Diversification Analysis. Our timetree of 217 species (Fig. S1) captures splitting events in the early history of major vertebrate lineages but provides little resolution within these lineages. However, the taxonomic richness of major vertebrate clades is among the best-characterized of all animal groups because of a long history of intensive study. We analyzed patterns of gnathostome diversification using MEDUSA, a comparative method that integrates phylogenetic information about the timing of splits along the backbone of a tree with taxonomic richness data to estimate rates of speciation and extinction. First, we pruned the 217-taxon timetree down to 47 tips representing major taxonomic divisions among jawed vertebrates. We attempted to resolve taxonomic groups to the lowest level that our 217-taxon tree would allow subject to 2 constraints imposed by the analysis. First, tips had to represent taxonomic groups that were monophyletic and nonnested. Second, the entirety of gnathostome species richness had to be completely partitioned among the represented taxonomic groups. We compiled species richness data from several sources including Nelson's Fishes of the World (39), the TIGR Reptile Database (40), the Mammal Species of the World database (http://nmnhgoph.si.edu/msw/), and others (41–43) (Table S4).

We used R (44) to perform all diversification analyses using the following libraries: Ape (45), Geiger (46), and Laser (47). R code to perform MEDUSA has been added to the Geiger library. To carry out these analyses, we fit BD models to the combined phylogenetic and taxonomic dataset (Fig. 1) using equations from Rabosky (13). Briefly, this method finds the likelihood of obtaining the particular combination of phylogenetic relationships (the tree with branch lengths) and taxonomic data (ages and species richnesses of extant groups) given particular values of b and d. We then calculate the AIC score for this model using the standard formula AIC = $2k - 2\ln L$, where k is the number of parameters needed to describe the model. MEDUSA starts by finding the maximum-likelihood values of b and d. This model is the starting point for the stepwise AIC algorithm.

Next, we fit a series of alternative models of increasing complexity, stopping when the improvement in AIC score is <4 [the threshold for a significant increase in model fit (16)]. For example, the first of these models includes a single breakpoint on one branch in the tree. The clade in the tree descended from this branch has its own set of birth and death rates (b1 and d1), whereas the remainder of the tree can potentially have different rates (b2 and d2). In some cases, the selected clade will include subclades with different rates assigned at earlier steps in the algorithm; in these cases, the subclade retains its distinct rates. For each possible branch, we find the maximum-likelihood values for all of the b and d parameters. We then calculate the AIC score, counting one parameter for each independent b and d rate, and one parameter for each branch selected as the location of a breakpoint. For example, a phylogenetic tree with a single breakpoint specifies a 5-parameter model: 2 birth rates, 2 death rates, and 1 branch where a change in rates occurs. We then select the breakpoint that minimizes this score. This represents a candidate for the next model to be kept; if the AIC score for this model is $\geq$4 units lower than the previous one, which had 2 fewer parameters, it is retained, and the process is continued. Currently, our method assumes that rates change instantaneously at the shift point; alternative models (such as models of correlated change through time) could also be implemented. When the AIC score for the best breakpoint is not less than some threshold number of AIC units smaller than the score for the previous model, the procedure is stopped, and the previous model is retained. We then apply a backwards elimination procedure where breakpoints are individually removed and the resulting model evaluated. If any of these simple models have a lower AIC score than the previous, they are retained, and the procedure repeated. After both the forward selection and backward elimination procedures are complete, one has a single model that identifies the simplest explanation, in terms of BD models with breakpoints, for the pattern of diversification in the clade.

More severe or relaxed AIC thresholds affect the number of rate shifts accepted for the final model and thus the identification of vertebrate clades as exceptional. These are explored in *SI Text*.

ACKNOWLEDGMENTS. We thank Gene Hunt, Pete Wagner, and John Alroy for critical discussions. Jonathan Losos, Arne Mooers and 2 anonymous reviewers provided helpful comments on earlier versions of this manuscript. This proposal was supported by the National Science Foundation (Grants DEB 0445453, DEB 071700, and DEB 0842397). Development of MEDUSA was partially supported by a NESCent Comparative Methods in R Hackathon.

1. Mooers AO, Heard SB (1997) Inferring evolutionary process from the phylogenetic tree shape. *Q Rev Biol* 72:31–54.
2. Slowinski JB, Guyer C (1993) Testing whether certain traits have caused amplified diversification: an improved method based on a model of random speciation and extinction. *Am Nat* 142:1019.
3. Schluter D (2000) *The Ecology of Adaptive Radiation* (Oxford Univ Press, New York).
4. Eldredge N, Stanley SM (1984) *Living Fossils* (Springer, New York).
5. Stanley SM (1979) *Macroevolution: Pattern and Process* (Freeman, San Francisco).
6. Raup DM, Gould SJ, Schopf TJM, Simberloff DS (1973) Stochastic models of phylogeny and the evolution of diversity. *J Geol* 81:525–542.
7. Bininda-Emonds OR, et al. (2007) The delayed rise of present-day mammals. *Nature* 446:507–512.

8. Ricklefs RE, Losos JB, Townsend TM (2007) Evolutionary diversification of clades of squamate reptiles. *J Evol Biol* 20:1751–1762.
9. Roelants K, et al. (2007) Global patterns of diversification in the history of modern amphibians. *Proc Natl Acad Sci USA* 104:887–892.
10. Chan KM, Moore BR (2005) SYMMETREE: Whole-tree analysis of differential diversification rates. *Bioinformatics* 21:1709–1710.
11. Chan KM, Moore BR (2002) Whole-tree methods for detecting differential diversification rates. *Syst Biol* 51:855–865.
12. Nee S, May RM, Harvey PH (1994) The reconstructed evolutionary process. *Phil Trans R Soc London, Ser B* 344:305–311.
13. Rabosky DL, Donnellan SC, Talaba AL, Lovette IJ (2007) Exceptional among-lineage variation in diversification rates during the radiation of Australia's most diverse vertebrate clade. *Proc Biol Sci* 274:2915–2923.
14. Woodburne MO, Rich TH, Springer MS (2003) The evolution of tribospheny and the antiquity of mammalian clades. *Mol Phylogenet Evol* 28:360–385.
15. Ostrom JH (1979) Bird flight: How did it begin? *Am Sci* 67:45–56.
16. Burnham KP, Anderson DR (2003) *Model Selection and Multimodel Inference, A Practical Information-Theoretic Approach* (Springer, New York).
17. Simpson GG (1944) *Tempo and Mode in Evolution* (Columbia Classics in Evolution Series) (Columbia Univ Press, New York), reprint Ed, 1984.
18. Darwin C (1859) *On the Origin of Species–A Facsimile of the First Edition* (Harvard Univ Press, Cambridge, MA).
19. Liow LH (2007) Lineages with long durations are old and morphologically average: An analysis using multiple datasets. *Evolution* 61:885–901.
20. Ricklefs RE (2005) Small clades at the periphery of passerine morphological space. *Am Nat* 165:651–659.
21. Strathmann RR, Slatkin M (1983) The improbability of animal phyla with few species. *Paleobiology* 9:97–106.
22. Evans SE, Chure D (1998) Paramacellodid lizard skulls from the Jurassic Morrison Formation at Dinosaur National Monument. *Utah J Vert Paleont* 18:99–114.
23. Forey PL (1998) *History of the Coelacanth Fishes* (Springer, London).
24. Markwick PJ (1998) Crocodilian diversity in space and time; the role of climate in paleoecology and its implication for understanding K/T extinctions. *Paleobiology* 24:470–497.
25. Grande L, Bemis W (1998) *A Comprehensive Phylogenetic Study of Amiid Fishes (Amiidae) Based on Comparative Skeletal Anatomy: An Empirical Search for Interconnected Patterns of Natural History (Memoir)* (Society of Vertebrate Paleontology, Lawrence, KS).
26. Etienne RS, Apol ME (2009) Estimating speciation and extinction rates from diversity data and the fossil record. *Evolution* 63:244–255.
27. Alroy J (2009) in *Speciation and Patterns of Diversity* (Cambridge Univ Press, Cambridge, MA), pp 301–323.
28. Nee S, Holmes EC, May RM, Harvey PH (1994) Extinction rates can be estimated from molecular phylogenies. *Philos Trans R Soc London Ser B* 344:77–82.
29. Paradis E (2004) Can extinction rates be estimated without fossils? *J Theor Biol* 229:19–30.
30. Rabosky DL (2009) Ecological limits on clade diversification in higher taxa. *Am Nat* 173:662–674.
31. Li C, Orti G (2007) Molecular phylogeny of Clupeiformes (Actinopterygii) inferred from nuclear and mitochondrial DNA sequences. *Mol Phylogenet Evol* 44:386–398.
32. Hugall AF, Foster R, Lee MS (2007) Calibration choice, rate smoothing, and the pattern of tetrapod diversification according to the long nuclear gene RAG-1. *Syst Biol* 56:543–563.
33. Brinkmann H, Venkatesh B, Brenner S, Meyer A (2004) Nuclear protein-coding genes support lungfish and not the coelacanth as the closest living relatives of land vertebrates. *Proc Natl Acad Sci USA* 101:4900–4905.
34. Townsend TM, Larson A, Louis E, Macey JR (2004) Molecular phylogenetics of Squamata: The position of snakes, Amphisbaenians, and Dibamids, and the root of the Squamate tree. *Syst Biol* 53:735–757.
35. Schluter SF, Marchalonis JJ (2003) Cloning of shark RAG2 and characterization of the *RAG1*/RAG2 gene locus. *FASEB J* 17:470–472.
36. Venkatesh B, Erdmann MV, Brenner S (2001) Molecular synapomorphies resolve evolutionary relationships of extant jawed vertebrates. *Proc Natl Acad Sci USA* 98:11382.
37. Thompson JD, Higgins DG, Gibson TJ (1994) CLUSTAL W: Improving the sensitivity of progressive multiple sequence alignment through sequence weighting, position-specific gap penalties and weight matrix choice. *Nucleic Acids Res* 22:4673–4680.
38. Drummond AJ, Rambaut (2007) A BEAST: Bayesian evolutionary analysis by sampling trees. *BMC Evol Biol* 7:214.
39. Nelson JS (2006) *Fishes of the World* (Wiley, Hoboken, NJ).
40. Uetz P, et al., *The Reptile Database*, http://www.reptile-database.org, accessed May 23, 2006.
41. Gill FG (2006) *Ornithology* (Freeman, New York).
42. Frost DR, Duellman WE (1985) *Amphibian Species of the World : A Taxonomic and Geographical Reference* (Allen/Association of Systematics Collections, Lawrence, KS).
43. Wilson DE, Reeder DAM (2005) Mammal Species of the World: A Taxonomic and Geographic Reference (Johns Hopkins Univ Press, Baltimore).
44. R Development Core Team (2005) R: A language and environment for statistical computing. R Foundation for Statistical Computing, Vienna, Austria. ISBN 3-900051-07-0, www.R-project.org.
45. Paradis E, Claude J, Strimmer K (2004) APE: Analyses of phylogenetics and evolution in R language. *Bioinformatics* 20:289–290.
46. Harmon LJ, Weir JT, Brock CD, Glor RE, Challenger W (2008) GEIGER: Investigating evolutionary radiations. *Bioinformatics* 24:129–131.
47. Rabosky DL (2006) LASER: A maximum likelihood toolkit for detecting temporal shifts in diversification rates from molecular phylogenies. *Evol Bioinformatics* 2:257–260.